行政院國家科學委員會專題研究計畫 成果報告

動態類神經網路在非線性系統鑑別與控制器設計之應用
研究成果報告(精簡版)

計 畫 類 別 ：個別型
計 畫 編 號 ：NSC 98-2221-E-009-126-
執 行 期 間 ：98 年 08 月 01 日至 99 年 07 月 31 日
執 行 單 位 ：國立交通大學電機與控制工程學系（所）

計 畫 主 持 人：王啟旭

計畫參與人員：碩士班研究生-兼任助理人員：黃繼輝
博士班研究生-兼任助理人員：洪&amp；#22531；能

報 告 附 件 ：出席國際會議研究心得報告及發表論文

處 理 方 式 ：本計畫可公開查詢

中 華 民 國 99 年 12 月 23 日

行政院國家科學委員會補助專題研究計畫 ☑ 成 果 報 告 □ 期中進度報告

動態類神經網路在非線性系統鑑別與控制器設計之應用

Application of Dynamic Neural Network Model for Nonlinear System Identification and Control

計畫類別：☑ 個別型計畫　　□ 整合型計畫

計畫編號：NSC 98-2221-E-009-126-

執行期間：　98　年　8　月　1　日至　99　年　7　月　31　日

計畫主持人：王啟旭
共同主持人：
計畫參與人員：

成果報告類型(依經費核定清單規定繳交)：☑精簡報告　□完整報告

本成果報告包括以下應繳交之附件：
□赴國外出差或研習心得報告一份
□赴大陸地區出差或研習心得報告一份
□出席國際學術會議心得報告及發表之論文各一份
□國際合作研究計畫國外研究報告書一份

處理方式：除產學合作研究計畫、提升產業技術及人才培育研究計畫、列管計畫及下列情形者外，得立即公開查詢
□涉及專利或其他智慧財產權，□一年□二年後可公開查詢

執行單位：**國立交通大學 電機工程學系**

中　華　民　國　九十九　年　十　月　十四　日

Application of Dynamic Neural Network Model for Nonlinear System Identification and Control

Abstract

The Hopfield neural network (HNN) has been widely discussed for controlling a nonlinear dynamical system. The weighting factors in HNN will be tuned via the Lyapunov stability criterion to guarantee the convergence performance. The proposed architecture in this paper is high-order Hopfield-based neural network (HOHNN), in which additional inputs from functional link net for each neuron are considered. Compared to HNN, the HOHNN performs faster convergence rate. The simulation results for both HNN and HOHNN show the effectiveness of HOHNN controller for affine nonlinear system. It is obvious from the simulation results that the performance for HOHNN controller is better than HNN controller.

1. Introduction

The Hopfield neural network (HNN) consists of a set of neuron and a corresponding set of unit delays forming a multiple-loop feedback system where the number of feedback loops is equal to the number of neurons. The HNN proposed in 1982 [1] has been adopted for pattern recognition [2], and image processing [3] in recent years. Neural networks, like HNNs, are suitable for controlling nonlinear dynamical systems due to their learning and memorizing capabilities.

Functional link net methodology was first proposed in 1989 [4, 5] which have been combined with the neural network to create the high-order neural networks (HONNs). The input pattern of a functional link net an expansion of original input variables in HNN. There have been many considerable interests in exploring the applications of functional link model to deal with nonlinearity and uncertainties. The advantages of high-order functional link net have been shown in [6], in which the efficiency of supervised learning is not only greatly improved, but a flat net without hidden layer is also capable enough of doing the same job. However the functional link neural networks in [7] does not include the Hopfield neural network (HNN), and the weighting factors tuned via back-propagation algorithm can not guarantee the convergence of the nonlinear dynamical systems, especially in the real-time applications.

In this paper, a new high-order Hopfield-based neural network (HOHNN) is proposed. It is basically a HNN with the compact functional link net and its exact analytical expression is also proposed. The application of HOHNN controller is explored in this paper to show the advantages of extra inputs for each neuron in HOHNN. A Lyapunov-based tuning algorithm is then proposed to find the optimal weighting matrix of HOHNN controller to achieve favorable approximation error. Furthermore, the convergence analysis with tuning weighting factors in the HOHNN controller is

considered. The simulation results for both HNN and HOHNN controllers are finally conducted to show that the HOHNN controller has better effective performance for nonlinear dynamical system than HNN controller.

2. Hopfield-based Network Models

Based on their feedback link connection architecture, there are three different types of artificial neural networks. We focus attention on the recurren Hopfield-based neural network in this paper. Considering the noiseless dynamic model of a single neuron in HNN illustrated in Fig. 1, the input vector $x^i(t) = [x_1^i(t) \quad x_2^i(t) \quad \dots \quad x_n^i(t)]$ represent voltages, the weighting vector $w^i(t) = [w_1^i(t) \quad w_2^i(t) \quad \dots \quad w_n^i(t)]$ represent conductance, and n represents the number of neurons. The input vector $x^i(t)$ are fed back from the output vector $y(t) = [y_1(t) \quad y_2(t) \quad \dots \quad y_n(t)]$, and a current source I_i represents the externally applied bias.

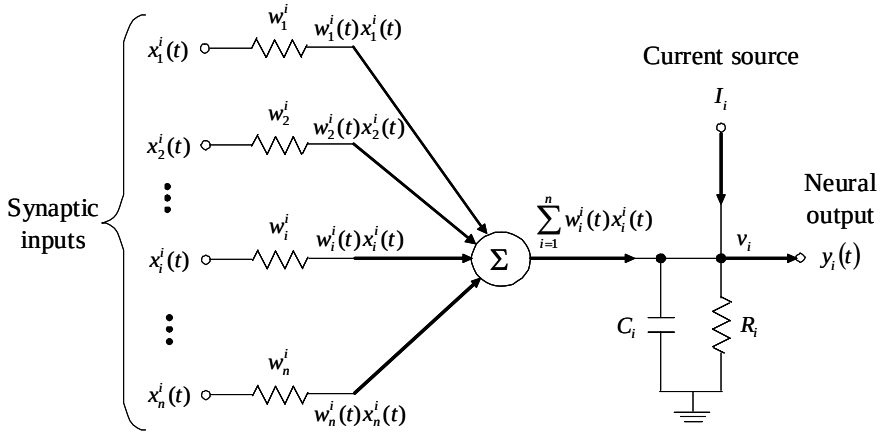

Fig. 1. The ith neuron in a Hopfield neural network.

The nonlinear function $\varphi(\cdot)$ is a sigmoid function which limits the amplitude range of the sum of inputs is defined by hyperbolic tangent function:

$$\varphi(v_i) = \tanh\left(\frac{a_i v_i}{2}\right) \tag{1}$$

where $a_i > 0$ refers to the gain of i^{th} neuron. By the Kirchhoff's current law, the following dynamic node equation can be obtained:

$$C_i \frac{dv_i(t)}{dt} + \frac{v_i(t)}{R_i} = \sum_{i=1}^{n} w^i(t) x^i(t) + I_i, \quad i = 1, \cdots, n. \tag{2}$$

Since the input is the feedback of the combination of output, (2) becomes

$$C_i \frac{dv_i(t)}{dt} + \frac{v_i(t)}{R_i} = \sum_{i=1}^{n} w^j(t)\varphi(v_i(t)) + I_i, \quad i = 1, \cdots, n. \tag{3}$$

The stability analysis of the above HNN has been proved in [8], in which an energy function was defined and it derivative function can be shown to be negative to yield an asymptotical stable system.

3. The Compact Functional Link Net with HNN

The functional link net is a single layer structure in which the hidden layer is removed. However, such functional transforms greatly increases the dimensions of input vector. Hence, it was suggested in [4] that high-order terms beyond the second-order term are not required in the enhanced patterns of input vector and the terms with two or more equal indices are also omitted. Therefore, a compact functional link net can be defined with rigorous formulae as shown in the following Fig. 2 and equations. The input pattern vector **Z** in Fig. 2 can be defined precisely as follows:

$$\mathbf{Z} = \begin{bmatrix} z_1 & z_2 & \cdots & z_N & z_{N+1} & \cdots & z_{\frac{N(N+1)}{2}} \end{bmatrix} \tag{4}$$

and

$$\begin{aligned}
&\left\{ z_{N+\ell_1} = z_1 z_{\ell_1+1} \quad | \quad \ell_1 = 1,2,..., N-1 \right\} \\
&\left\{ z_{(2N-1)+\ell_2} = z_2 z_{\ell_2+2} \quad | \quad \ell_2 = 1,2,..., N-2 \right\} \\
&\cdots \\
&\left\{ z_{\left[kN - \frac{k(k-1)}{2}\right]+\ell_4} = z_k z_{\ell_k+k} \quad | \quad \ell_k = 1,2,..., N-k \right\} \\
&\cdots \\
&\left\{ z_{\left[(N-1)N - \frac{(N-1)(N-2)}{2}\right]+\ell_{N-1}} = z_{N-1} z_{\ell_{N-1}+N-1} \quad | \quad \ell_{N-1} = 1,2,..., N-(N-1) \right\}.
\end{aligned} \tag{5}$$

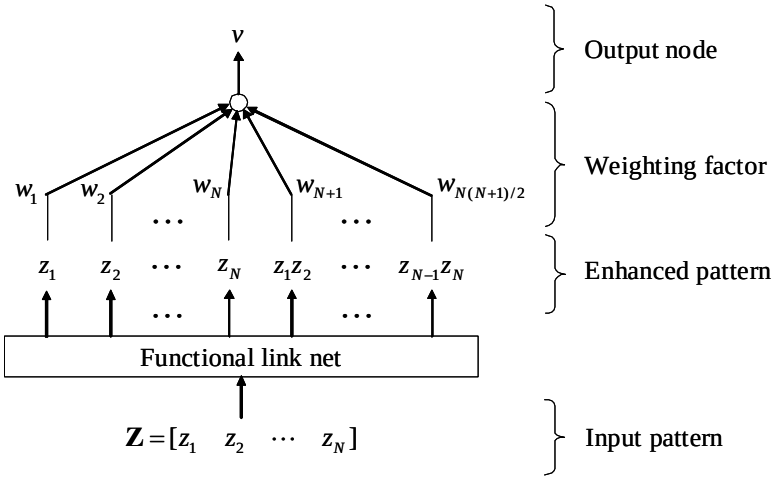

Fig. 2. A compact structure of functional link net.

Equation (4) says that the dimension of **Z** vector is $N\ (N + 1) / 2$, in which N is the number of original input variables. All the extra second order terms in (5) for $\left\{ z_{N+1} \quad z_{N+2} \quad \cdots \quad z_{\frac{N(N+1)}{2}} \right\}$ are described. Further we let the input vector of HNN in Fig. 1 to form a compact functional link net defined in Fig. 2. This combination in HOHNN structure for a single neuron is shown in the following Fig. 3.

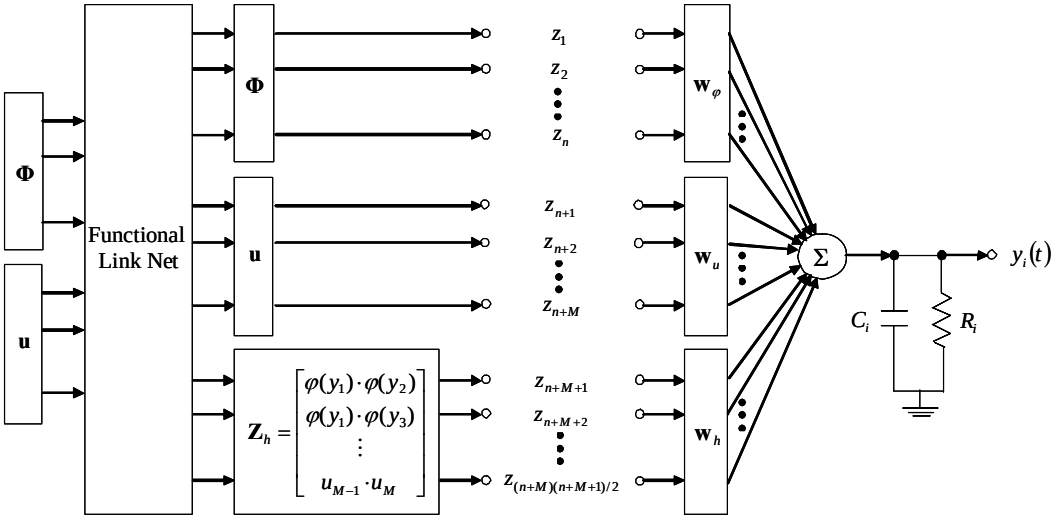

Fig. 3. The high-order HNN (HOHNN) for a single neuron.

The input pattern of HOHNN produced from functional link net is the enhanced pattern in which $\mathbf{\Phi}$ is the n-dimension vector of the network feedback, **u** is the M-dimension vector of the input; and $\mathbf{Z}_h$ is the high-order term vectors to the system in Fig. 3. For this compact functional link net, the dimension of input vector has been expanded to $N = (n + M)\ (n + M + 1) / 2$. Thus, the N-dimension input vector **Z** and the $n \times N$ matrix of weighting factor matrix can be defined as

$$\mathbf{Z} = \left[\mathbf{\Phi} \quad \mathbf{u} \quad \mathbf{Z}_h \right]^T \tag{6}$$

and

$$\mathbf{W} = [\mathbf{w}_\varphi \quad \mathbf{w}_u \quad \mathbf{w}_h] \tag{7}$$

where $\mathbf{w}_\varphi$, $\mathbf{w}_u$, and $\mathbf{w}_h$ represent the weighting factors of feedback input, error input and high-order term, respectively.

4. The HOHNN Controller for Nonlinear System

The structure of HOHNN in Fig. 4 can be expressed as

$$\dot{\mathbf{x}} = \mathbf{A}\mathbf{x} + \mathbf{B}\mathbf{w}_{\varphi}{}^{T}\mathbf{\Phi} + \mathbf{B}\mathbf{w}_{u}{}^{T}\mathbf{u} + \mathbf{B}\mathbf{w}_{h}{}^{T}\mathbf{Z}_{h}. \tag{8}$$

where $\mathbf{A} = diag\{-a_1 \quad -a_2 \quad \cdots \quad -a_n\} \in R^{n\times n}$ is a Hurwitz matrix with $a_i = 1/(R_i C_i)$; and $\mathbf{B} = diag\{b_1 \quad b_2 \quad \cdots \quad b_n\} \in R^{n\times n}$ with $b_i = 1/C_i$. The output of each neuron in HOHNN can be expressed as

$$\dot{x}_i = -a_i x_i + b_i \mathbf{w}_{\varphi,i}{}^{T}\mathbf{\Phi} + b_i \mathbf{w}_{u,i}{}^{T}\mathbf{u} + b_i \mathbf{w}_{h,i}{}^{T}\mathbf{Z}_h, \quad i = 1,2,\ldots,n \tag{9}$$

where $\mathbf{w}_{\varphi,i}{}^{T}$, $\mathbf{w}_{u,i}{}^{T}$, and $\mathbf{w}_{h,i}{}^{T}$ are the i^{th} rows of $\mathbf{w}_{\varphi}$, $\mathbf{w}_{u}$, and $\mathbf{w}_{h}$, respectively. Solve the differential equation (8), we obtain

$$\begin{aligned} x_i &= b_i(\mathbf{w}_{\varphi,i}{}^{T}\zeta_{\varphi,i} + \mathbf{w}_{u,i}{}^{T}\zeta_{u,i} + \mathbf{w}_{h,i}{}^{T}\zeta_{h,i}) + e^{-a_i t}x_i{}^{0} \\ &- e^{-a_i t}b_i(\mathbf{w}_{\varphi,i}{}^{T}\zeta_{\varphi,i}{}^{0} + \mathbf{w}_{u,i}{}^{T}\zeta_{u,i}{}^{0} + \mathbf{w}_{h,i}{}^{T}\zeta_{h,i}{}^{0}), i = 1,2,\ldots,n \end{aligned} \tag{10}$$

where $x_i{}^{0}$ is the initial state of x_i; $\zeta_{\varphi,i} \in R^{n}$, $\zeta_{u,i} \in R^{M}$, and $\zeta_{h,i} \in R^{(n+M)(n+M-1)/2}$ are the solutions of $\dot{\zeta}_{\varphi,i} = -a_i\zeta_{\varphi,i} + \mathbf{\Phi}$, $\dot{\zeta}_{u,i} = -a_i\zeta_{u,i} + \mathbf{u}$, and $\dot{\zeta}_{h,i} = -a_i\zeta_{h,i} + \mathbf{Z}_h$, respectively; $\zeta_{\varphi,i}{}^{0}$, $\zeta_{u,i}{}^{0}$, and $\zeta_{h,i}{}^{0}$ are initial states of $\zeta_{\varphi,i}$, $\zeta_{u,i}$, and $\zeta_{h,i}$, respectively. Note that $e^{-a_i t}x_i{}^{0}$ and $e^{-a_i t}b_i(\mathbf{w}_{\varphi,i}{}^{T}\zeta_{\varphi,i}{}^{0} + \mathbf{w}_{u,i}{}^{T}\zeta_{u,i}{}^{0} + \mathbf{w}_{h,i}{}^{T}\zeta_{h,i}{}^{0})$ in (10) will exponentially decay with time due to the fact $a_i > 0$.

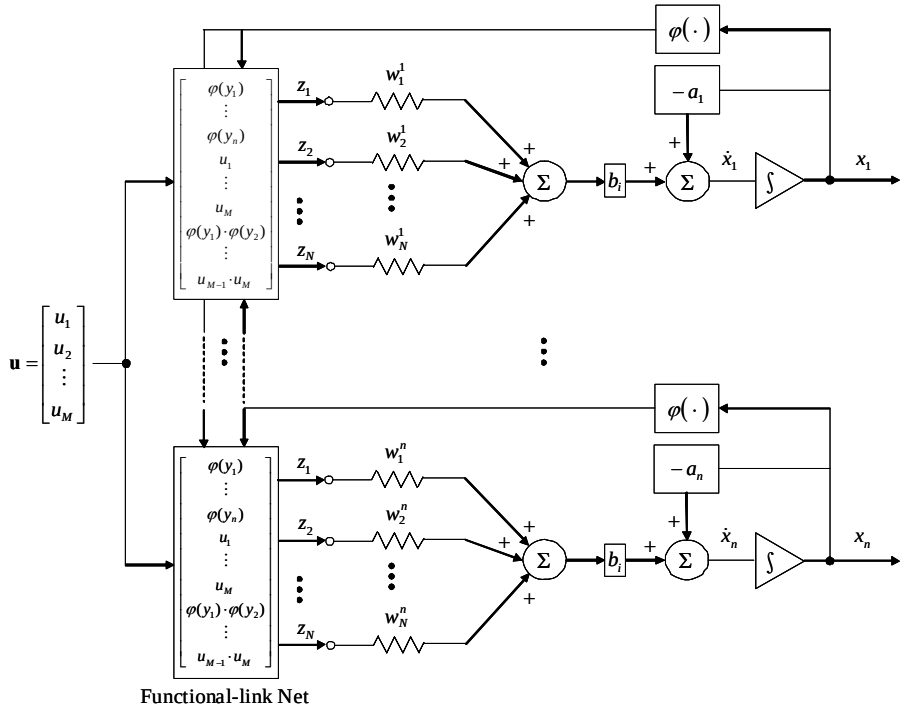

Fig. 4. The structure of HOHNN.

Consider the n^{th}-order nonlinear dynamical system of the following form:

$$\begin{aligned} x^{(n)} &= f(\mathbf{x}) + gu + d \\ y &= x \end{aligned} \tag{11}$$

where $\mathbf{x} = [x_1 \quad x_2 \quad \cdots \quad x_n]^T$ is the system state vector, the nonlinear function $f : R^n \to R$ describes the system dynamics, $u \in R$ is a continuous control input of the system, and $d \in R$ is a bounded external disturbance. In order for (11) to be controllable and without losing generality, it is required that $0 < g < \infty$. The control objective is to force the system output y to follow a given bounded reference signal y_r. The reference signal vector $\mathbf{y}_r$ and the error vector **e** are defined as

$$\mathbf{e} = [e, \dot{e}, \ldots, e^{(n-1)}]^T \in R^n \tag{12}$$

with $e = y_r - x = y_r - y$. If the function $f(\mathbf{x})$ and g are known and the system is free of external disturbance, the ideal controller can be designed as

$$u_{ideal} = \frac{1}{g}[-f(\mathbf{x}) + y_r^{(n)} + \mathbf{k}_c{}^T \mathbf{e}]^T \tag{13}$$

where $\mathbf{k}_c = [k_n, k_{n-1}, \ldots, k_1]^T$. Applying (13) to (11), we have the following error dynamical system

$$e^{(n)} + k_1 e^{(n-1)} + \cdots + k_n e = 0 \tag{14}$$

If $k_i, i = 1,2,\ldots,n$ are chosen so that all roots of the polynomial

$H(s) \cong s^n + k_1 s^{n-1} + \cdots + k_n$ lie strictly in the left half of the complex plane, then $\lim_{t\to\infty} e(t) = 0$ can be implied for any initial conditions. However, since the system dynamics may be unknown or perturbed, the ideal controller u_{ideal} in (13) cannot be implemented. In order to control the unknown nonlinear system, an HOHNN with single layer, fully connection, recurrent nets and functional link model is proposed. The overall closed-loop diagram of direct adaptive HOHNN controller for affine nonlinear system is shown in the following Fig. 5.

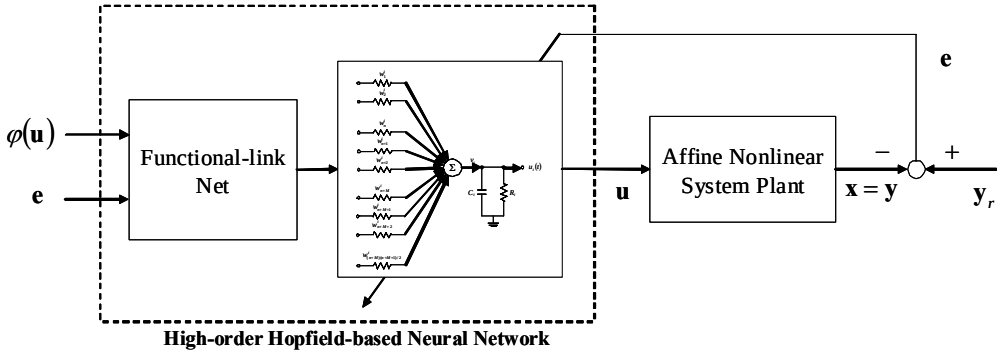

Fig. 5. The closed-loop configuration of HOHNN controller for affine nonlinear system.

Substituting $u = u_{ideal}$ into (11) and using (13) yields

$$\dot{\mathbf{e}} = \mathbf{A}\mathbf{e} + g\mathbf{B}(u_{ideal} - u) - \mathbf{B}d = \mathbf{A}\mathbf{e} + g\mathbf{B}\tilde{u} - \mathbf{B}d \tag{15}$$

where $\mathbf{A} = \begin{bmatrix} 0 & 1 & 0 & \cdots & 0 \\ \vdots & \ddots & \ddots & \ddots & 0 \\ 0 & 0 & \cdots & 0 & 1 \\ -k_n & -k_{n-1} & -k_{n-2} & \cdots & -k_1 \end{bmatrix}_{n\times n}$, $\mathbf{B} = \begin{bmatrix} 0 \\ 0 \\ \vdots \\ 1 \end{bmatrix}_{n\times 1}$, and $\tilde{u} = u_{ideal} - u$. Note that the ideal controller u_{ideal} is a scalar, and thus the HOHNN controller contains only a single neuron. The input signals shown in the HOHNN controller shown in Fig. 3 are

$$\mathbf{\Phi} = \begin{bmatrix} \varphi(u_1) & \varphi(u_2) & \cdots & \varphi(u_n) \end{bmatrix}^T,$$

$$\mathbf{u} = \begin{bmatrix} e_1 & e_2 & \cdots & e_M \end{bmatrix}^T = \begin{bmatrix} e & \dot{e} & \cdots & e^{(M-1)} \end{bmatrix}^T,$$

and

$$\mathbf{Z}_h = \begin{bmatrix} \varphi(u_1)\cdot\varphi(u_2) & \cdots & \varphi(u_1)\cdot\varphi(u_n) & \cdots & \cdots & e_{M-1}\cdot e_M \end{bmatrix}^T. \tag{16}$$

where $\mathbf{Z}_h$ vector in (16) comes from (5) in the compact functional link net shown in Fig. 2. The output signal can be expressed as

$$u = \frac{1}{C}(\hat{\mathbf{w}}_\varphi \zeta_\varphi + \hat{\mathbf{w}}_u \zeta_u + \hat{\mathbf{w}}_h \zeta_h) + e^{-\frac{1}{RC}t} u^0 - e^{-\frac{1}{RC}t} \frac{1}{C}(\hat{\mathbf{w}}_\varphi \zeta_\varphi{}^0 + \hat{\mathbf{w}}_u \zeta_u{}^0 + \hat{\mathbf{w}}_h \zeta_h{}^0). \quad (17)$$

where u^0 is the initial value of u; $\hat{\mathbf{w}}_\varphi$, $\hat{\mathbf{w}}_\varphi$, and $\hat{\mathbf{w}}_\varphi$ are the estimations of $\mathbf{w}_\varphi$, $\mathbf{w}_\varphi$, and $\mathbf{w}_\varphi$. Substituting (17) into (15) yields

$$\dot{\mathbf{e}} = \mathbf{A}\mathbf{e} + g\mathbf{B}\left[\frac{1}{C}\tilde{\mathbf{w}}_\varphi\left(\zeta_\varphi - e^{-\frac{1}{RC}t}\zeta_\varphi{}^0\right) + \frac{1}{C}\tilde{\mathbf{w}}_u\left(\zeta_u - e^{-\frac{1}{RC}t}\zeta_u{}^0\right) + \frac{1}{C}\tilde{\mathbf{w}}_h\left(\zeta_h - e^{-\frac{1}{RC}t}\zeta_h{}^0\right) + \Delta\right] - \mathbf{B}d \quad (18)$$

where Δ is the control error. In order to derive the one of main theorems in the following section, the following assumption is required.

Assumption: Let $\varepsilon = \Delta - \frac{1}{g}d$. Assume that there exists a finite constant μ so that

$$\int_0^t \varepsilon^2 d\tau \le \mu, \quad 0 \le t < \infty. \quad (19)$$

The constraint set for $\hat{\mathbf{w}}_\varphi$, $\hat{\mathbf{w}}_u$, and $\hat{\mathbf{w}}_h$ are $\mathbf{\Omega}_\varphi = \{\hat{\mathbf{w}}_\varphi : \|\hat{\mathbf{w}}_\varphi\| \le M_{\mathbf{w}_\varphi}\}$, $\mathbf{\Omega}_u = \{\hat{\mathbf{w}}_u : \|\hat{\mathbf{w}}_u\| \le M_{\mathbf{w}_u}\}$, and $\mathbf{\Omega}_h = \{\hat{\mathbf{w}}_h : \|\hat{\mathbf{w}}_h\| \le M_{\mathbf{w}_h}\}$. If the adaptive laws are designed as

$$\dot{\hat{\mathbf{w}}}_\varphi = -\dot{\tilde{\mathbf{w}}}_\varphi = \begin{cases} \frac{\beta_\varphi}{C}\mathbf{e}^T\mathbf{P}\mathbf{B}\left(\zeta_\varphi - e^{-\frac{1}{RC}t}\zeta_\varphi{}^0\right) & \text{if } \left(\|\hat{\mathbf{w}}_\varphi\| < M_{\mathbf{w}_\varphi}\right) \text{or} \left(\|\hat{\mathbf{w}}_\varphi\| = M_{\mathbf{w}_\varphi} \text{ and } \mathbf{e}^T\mathbf{P}\mathbf{B}\hat{\mathbf{w}}_\varphi\left(\zeta_\varphi - e^{-\frac{1}{RC}t}\zeta_\varphi{}^0\right) \ge 0\right) \\ \mathbf{Pr}\left[\frac{\beta_\varphi}{C}\mathbf{e}^T\mathbf{P}\mathbf{B}\left(\zeta_\varphi - e^{-\frac{1}{RC}t}\zeta_\varphi{}^0\right)\right] & \text{if } \left(\|\hat{\mathbf{w}}_\varphi\| = M_{\mathbf{w}_\varphi} \text{ and } \mathbf{e}^T\mathbf{P}\mathbf{B}\hat{\mathbf{w}}_\varphi\left(\zeta_\varphi - e^{-\frac{1}{RC}t}\zeta_\varphi{}^0\right) < 0\right) \end{cases} \quad (20)$$

$$\dot{\hat{\mathbf{w}}}_u = -\dot{\tilde{\mathbf{w}}}_u = \begin{cases} \frac{\beta_u}{C}\mathbf{e}^T\mathbf{P}\mathbf{B}\left(\zeta_u - e^{-\frac{1}{RC}t}\zeta_u{}^0\right) & \text{if } \left(\|\hat{\mathbf{w}}_u\| < M_{\mathbf{w}_u}\right) \text{or} \left(\|\hat{\mathbf{w}}_u\| = M_{\mathbf{w}_u} \text{ and } \mathbf{e}^T\mathbf{P}\mathbf{B}\hat{\mathbf{w}}_u\left(\zeta_u - e^{-\frac{1}{RC}t}\zeta_u{}^0\right) \ge 0\right) \\ \mathbf{Pr}\left[\frac{\beta_u}{C}\mathbf{e}^T\mathbf{P}\mathbf{B}\left(\zeta_u - e^{-\frac{1}{RC}t}\zeta_u{}^0\right)\right] & \text{if } \left(\|\hat{\mathbf{w}}_u\| = M_{\mathbf{w}_u} \text{ and } \mathbf{e}^T\mathbf{P}\mathbf{B}\hat{\mathbf{w}}_u\left(\zeta_u - e^{-\frac{1}{RC}t}\zeta_u{}^0\right) < 0\right) \end{cases} \quad (21)$$

$$\dot{\hat{\mathbf{w}}}_h = -\dot{\tilde{\mathbf{w}}}_h = \begin{cases} \frac{\beta_h}{C}\mathbf{e}^T\mathbf{P}\mathbf{B}\left(\zeta_h - e^{-\frac{1}{RC}t}\zeta_h{}^0\right) & \text{if } \left(\|\hat{\mathbf{w}}_h\| < M_{\mathbf{w}_h}\right) \text{or} \left(\|\hat{\mathbf{w}}_h\| = M_{\mathbf{w}_h} \text{ and } \mathbf{e}^T\mathbf{P}\mathbf{B}\hat{\mathbf{w}}_h\left(\zeta_h - e^{-\frac{1}{RC}t}\zeta_h{}^0\right) \ge 0\right) \\ \mathbf{Pr}\left[\frac{\beta_h}{C}\mathbf{e}^T\mathbf{P}\mathbf{B}\left(\zeta_h - e^{-\frac{1}{RC}t}\zeta_h{}^0\right)\right] & \text{if } \left(\|\hat{\mathbf{w}}_h\| = M_{\mathbf{w}_h} \text{ and } \mathbf{e}^T\mathbf{P}\mathbf{B}\hat{\mathbf{w}}_h\left(\zeta_h - e^{-\frac{1}{RC}t}\zeta_h{}^0\right) < 0\right) \end{cases} \quad (22)$$

where β_φ, β_u, and β_h are possible learning rates; the symmetric positive definite matrix **P** satisfies the following Riccati-like equation

$$\mathbf{A}^T\mathbf{P} + \mathbf{P}\mathbf{A} + \mathbf{Q} + \mathbf{P}\mathbf{B}\frac{1}{\rho^2}\mathbf{B}^T\mathbf{P} = 0 \quad (23)$$

where **Q** is a symmetric matrix and ρ is a constant; the projection operators **Pr**[*] are defined as

$$\mathbf{Pr}\left[\frac{\beta_\varphi}{C}\mathbf{e}^T\mathbf{PB}\left(\zeta_\varphi - e^{-\frac{1}{RC}t}\zeta_\varphi{}^0\right)\right] = \frac{\beta_\varphi}{C}\left[\mathbf{e}^T\mathbf{PB}\left(\zeta_\varphi - e^{-\frac{1}{RC}t}\zeta_\varphi{}^0\right) + \mathbf{e}^T\mathbf{PB}\frac{\hat{\mathbf{w}}_\varphi\left(\zeta_\varphi - e^{-\frac{1}{RC}t}\zeta_\varphi{}^0\right)}{\left\|\hat{\mathbf{w}}_\varphi\right\|^2}\hat{\mathbf{w}}_\varphi\right], \quad (24)$$

$$\mathbf{Pr}\left[\frac{\beta_u}{C}\mathbf{e}^T\mathbf{PB}\left(\zeta_u - e^{-\frac{1}{RC}t}\zeta_u{}^0\right)\right] = \frac{\beta_u}{C}\left[\mathbf{e}^T\mathbf{PB}\left(\zeta_u - e^{-\frac{1}{RC}t}\zeta_u{}^0\right) + \mathbf{e}^T\mathbf{PB}\frac{\hat{\mathbf{w}}_u\left(\zeta_u - e^{-\frac{1}{RC}t}\zeta_u{}^0\right)}{\left\|\hat{\mathbf{w}}_u\right\|^2}\hat{\mathbf{w}}_u\right], \quad (25)$$

and

$$\mathbf{Pr}\left[\frac{\beta_h}{C}\mathbf{e}^T\mathbf{PB}\left(\zeta_h - e^{-\frac{1}{RC}t}\zeta_h{}^0\right)\right] = \frac{\beta_h}{C}\left[\mathbf{e}^T\mathbf{PB}\left(\zeta_h - e^{-\frac{1}{RC}t}\zeta_h{}^0\right) + \mathbf{e}^T\mathbf{PB}\frac{\hat{\mathbf{w}}_h\left(\zeta_h - e^{-\frac{1}{RC}t}\zeta_h{}^0\right)}{\left\|\hat{\mathbf{w}}_h\right\|^2}\hat{\mathbf{w}}_h\right] \quad (26)$$

then $\hat{\mathbf{w}}_\varphi$, $\hat{\mathbf{w}}_u$, and $\hat{\mathbf{w}}_h$ are bounded by $\left\|\hat{\mathbf{w}}_\varphi\right\| \le M_{\mathbf{w}_\varphi}$, $\left\|\hat{\mathbf{w}}_u\right\| \le M_{\mathbf{w}_u}$, and $\left\|\hat{\mathbf{w}}_h\right\| \le M_{\mathbf{w}_h}$ for all $t \ge 0$ [9, 10].

Consider the Lyapunov candidate function as

$$V = \frac{1}{2}\mathbf{e}^T\mathbf{Pe} + \frac{1}{2\eta_\varphi}tr(\tilde{\mathbf{w}}_\varphi{}^T\tilde{\mathbf{w}}_\varphi) + \frac{1}{2\eta_u}tr(\tilde{\mathbf{w}}_u{}^T\tilde{\mathbf{w}}_u) + \frac{1}{2\eta_h}tr(\tilde{\mathbf{w}}_h{}^T\tilde{\mathbf{w}}_h) \quad (27)$$

where $\eta_\varphi = \frac{\beta_\varphi}{g}$, $\eta_u = \frac{\beta_u}{g}$ and $\eta_h = \frac{\beta_h}{g}$ are positive learning rates; $\tilde{\mathbf{w}}_\varphi = \mathbf{w}_\varphi{}^* - \hat{\mathbf{w}}_\varphi$, $\tilde{\mathbf{w}}_u = \mathbf{w}_u{}^* - \hat{\mathbf{w}}_u$, and $\tilde{\mathbf{w}}_h = \mathbf{w}_h{}^* - \hat{\mathbf{w}}_h$, where $\mathbf{w}_\varphi{}^*$, $\mathbf{w}_u{}^*$, and $\mathbf{w}_h{}^*$ are defined the optimal vectors. $\mathbf{P} > 0$ is chosen to satisfy the Lyapunov equation. Taking the derivative of V with respect to time and using (18) yields

$$\begin{aligned}\dot{V} &= \frac{1}{2}(\mathbf{e}^T\mathbf{P}\dot{\mathbf{e}} + \dot{\mathbf{e}}^T\mathbf{Pe}) + \frac{1}{\eta_\varphi}tr(\dot{\tilde{\mathbf{w}}}_\varphi{}^T\tilde{\mathbf{w}}_\varphi) + \frac{1}{\eta_u}tr(\dot{\tilde{\mathbf{w}}}_u{}^T\tilde{\mathbf{w}}_u) + \frac{1}{\eta_h}tr(\dot{\tilde{\mathbf{w}}}_h{}^T\tilde{\mathbf{w}}_h) \\ &= \frac{1}{2}\mathbf{e}^T(\mathbf{A}^T\mathbf{P} + \mathbf{PA})\mathbf{e} + g\mathbf{e}^T\mathbf{PB}\left(\Delta - \frac{1}{g}d\right) + V_\varphi + V_u + V_h\end{aligned} \quad (28)$$

where

$$V_\varphi = g\dot{\tilde{\mathbf{w}}}_\varphi{}^T\left[\frac{1}{C}\mathbf{e}^T\mathbf{PB}\left(\zeta_\varphi - e^{-\frac{1}{RC}t}\zeta_\varphi{}^0\right) + \frac{1}{\beta_\varphi}\tilde{\mathbf{w}}_\varphi\right], \quad (29)$$

$$V_u = g\dot{\tilde{\mathbf{w}}}^T{}_u\left[\frac{1}{C}\mathbf{e}^T\mathbf{PB}\left(\zeta_u - e^{-\frac{1}{RC}t}\zeta_u{}^0\right) + \frac{1}{\beta_u}\tilde{\mathbf{w}}_u\right], \quad (30)$$

and

$$V_h = g\tilde{\mathbf{w}}_h{}^T\left[\frac{1}{C}\mathbf{e}^T\mathbf{PB}\left(\zeta_h - e^{-\frac{1}{RC}t}\zeta_h{}^0\right) + \frac{1}{\beta_h}\tilde{\mathbf{w}}_h\right]. \tag{31}$$

Using the Riccati-like equation (23), (28) can be rewritten as

$$\begin{aligned}\dot{V} &= \frac{1}{2}\mathbf{e}^T\left(-\mathbf{Q} - \frac{1}{\rho^2}\mathbf{PBB}^T\mathbf{P}\right)\mathbf{e} + g\mathbf{e}^T\mathbf{PB}\varepsilon + V_\varphi + V_u + V_h \\ &= -\frac{1}{2}\mathbf{e}^T\mathbf{Qe} - \frac{1}{2}\left[\frac{1}{\rho}\mathbf{B}^T\mathbf{Pe} - g\rho\varepsilon\right]^2 + \frac{1}{2}g^2\rho^2\varepsilon^2 + V_\varphi + V_u + V_h.\end{aligned} \tag{32}$$

Using (20), we have

$$V_\varphi = \begin{cases} 0 & \text{if } \left(\left\|\hat{\mathbf{w}}_\varphi\right\| < M_{\mathbf{w}_\varphi}\right) \text{or} \left(\left\|\hat{\mathbf{w}}_\varphi\right\| = M_{\mathbf{w}_\varphi} \text{ and } \mathbf{e}^T\mathbf{PB}\hat{\mathbf{w}}_\varphi\left(\zeta_\varphi - e^{-\frac{1}{RC}t}\zeta_\varphi{}^0\right) \geq 0\right). \\ -\frac{g}{C}\mathbf{e}^T\mathbf{PB}\dfrac{\hat{\mathbf{w}}_\varphi{}^T\left(\zeta_\varphi - e^{-\frac{1}{RC}t}\zeta_\varphi{}^0\right)}{\left\|\hat{\mathbf{w}}_\varphi\right\|^2}\tilde{\mathbf{w}}_\varphi\hat{\mathbf{w}}_\varphi & \text{if } \left(\left\|\hat{\mathbf{w}}_\varphi\right\| = M_{\mathbf{w}_\varphi} \text{ and } \mathbf{e}^T\mathbf{PB}\hat{\mathbf{w}}_\varphi\left(\zeta_\varphi - e^{-\frac{1}{RC}t}\zeta_\varphi{}^0\right) < 0\right) \end{cases}. \tag{33}$$

For the conditions $\left\|\hat{\mathbf{w}}_\varphi\right\| = M_{\mathbf{w}_\varphi}$ and $\mathbf{e}^T\mathbf{PB}\hat{\mathbf{w}}_\varphi\left(\zeta_\varphi - e^{-\frac{1}{RC}t}\zeta_\varphi{}^0\right) < 0$, we have $\left\|\hat{\mathbf{w}}_\varphi\right\| = M_{\mathbf{w}_\varphi} \geq \left\|\mathbf{w}_\varphi{}^*\right\|$ because $\mathbf{w}_\varphi{}^*$ belongs to the constraint set $\mathbf{\Omega}_\varphi$. Using this fact, we obtain $\tilde{\mathbf{w}}_\varphi\hat{\mathbf{w}}_\varphi = \frac{1}{2}\left(\left\|\mathbf{w}_\varphi{}^*\right\|^2 - \left\|\hat{\mathbf{w}}_\varphi\right\|^2 - \left\|\tilde{\mathbf{w}}_\varphi\right\|^2\right) \leq 0$. Thus, the second line of (33) can be rewritten as

$$V_\varphi = -\frac{g}{2C}\mathbf{e}^T\mathbf{PB}\frac{\hat{\mathbf{w}}_\varphi{}^T\left(\zeta_\varphi - e^{-\frac{1}{RC}t}\zeta_\varphi{}^0\right)}{\left\|\hat{\mathbf{w}}_\varphi\right\|^2}\left(\left\|\mathbf{w}_\varphi{}^*\right\|^2 - \left\|\hat{\mathbf{w}}_\varphi\right\|^2 - \left\|\tilde{\mathbf{w}}_\varphi\right\|^2\right) \leq 0. \tag{34}$$

Similarly, we obtain

$$V_u = -\frac{g}{2C}\mathbf{e}^T\mathbf{PB}\frac{\hat{\mathbf{w}}_u{}^T\left(\zeta_u - e^{-\frac{1}{RC}t}\zeta_u{}^0\right)}{\left\|\hat{\mathbf{w}}_u\right\|^2}\left(\left\|\mathbf{w}_u{}^*\right\|^2 - \left\|\hat{\mathbf{w}}_u\right\|^2 - \left\|\tilde{\mathbf{w}}_u\right\|^2\right) \leq 0, \tag{35}$$

and

$$V_h = -\frac{g}{2C}\mathbf{e}^T\mathbf{PB}\frac{\hat{\mathbf{w}}_h{}^T\left(\zeta_h - e^{-\frac{1}{RC}t}\zeta_h{}^0\right)}{\left\|\hat{\mathbf{w}}_h\right\|^2}\left(\left\|\mathbf{w}_h{}^*\right\|^2 - \left\|\hat{\mathbf{w}}_h\right\|^2 - \left\|\tilde{\mathbf{w}}_h\right\|^2\right) \leq 0. \tag{36}$$

Using the knowledge that $V_\varphi \leq 0$, $V_u \leq 0$ and $V_h \leq 0$, we can further rewrite (32) as

$$\dot{V} \leq -\frac{1}{2}\mathbf{e}^T\mathbf{Qe} + \frac{1}{2}(\rho g\varepsilon)^2. \tag{37}$$

Integrating both sides of the inequality (37) yields

$$V(t)-V(0)\le -\frac{1}{2}\int_0^t \mathbf{e}^T\mathbf{Q}\mathbf{e}d\tau+\frac{g^2\rho^2}{2}\int_0^t \varepsilon^2 d\tau \quad \text{for} \quad 0\le t<\infty. \tag{38}$$

Since $V(t)\ge 0$, we obtain

$$\frac{1}{2}\int_0^t \mathbf{e}^T\mathbf{Q}\mathbf{e}d\tau\le V(0)+\frac{g^2\rho^2}{2}\int_0^t \varepsilon^2 d\tau. \tag{39}$$

Substituting (27) into (39), we can obtain

$$\frac{1}{2}\int_0^t \mathbf{e}^T\mathbf{Q}\mathbf{e}d\tau\le \frac{1}{2}\int_0^t \mathbf{e}_0{}^T\mathbf{P}\mathbf{e}_0+\frac{\tilde{\mathbf{w}}_{\varphi 0}\dot{\tilde{\mathbf{w}}}_{\varphi 0}}{2\eta_\varphi}+\frac{\tilde{\mathbf{w}}_{u0}\dot{\tilde{\mathbf{w}}}_{u0}}{2\eta_u}+\frac{\tilde{\mathbf{w}}_{h0}\dot{\tilde{\mathbf{w}}}_{h0}}{2\eta_h}+\frac{g^2\rho^2}{2}\int_0^t \varepsilon^2 d\tau \tag{40}$$

where $\mathbf{e}_0$, $\tilde{\mathbf{w}}_{\varphi 0}$, $\tilde{\mathbf{w}}_{u0}$, and $\tilde{\mathbf{w}}_{h0}$ are the initial values of $\mathbf{e}$, $\tilde{\mathbf{w}}_{\varphi}$, $\tilde{\mathbf{w}}_{u}$, and $\tilde{\mathbf{w}}_{h}$, respectively. From (39) and since $\int_0^t \mathbf{e}^T\mathbf{Q}\mathbf{e}d\tau\ge 0$, we have

$$2V(t)\le 2V(0)+g^2\rho^2\mu,\quad 0\le t<\infty. \tag{41}$$

where $V(0)$ is the initial value of a Lyapunov function candidate. From (27), it is obvious that $\mathbf{e}^T\mathbf{P}\mathbf{e}\le 2V$ for any V. Because $\mathbf{P}$ is a positive definite symmetric matrix, we have

$$\lambda_{\min}(\mathbf{P})\|\mathbf{e}\|^2=\lambda_{\min}(\mathbf{P})\mathbf{e}^T\mathbf{e}\le \mathbf{e}^T\mathbf{P}\mathbf{e}. \tag{42}$$

where $\lambda_{\min}(\mathbf{P})$ is the minimum eigenvalue of $\mathbf{P}$. Thus, from (41) and (42) we obtain

$$\lambda_{\min}(\mathbf{P})\|\mathbf{e}\|^2\le \mathbf{e}^T\mathbf{P}\mathbf{e}\le 2V(t)\le 2V(0)+g^2\rho^2\mu. \tag{43}$$

Therefore, the tracking error $\|\mathbf{e}\|$ can be expressed in terms of the lumped uncertainty as

$$\|\mathbf{e}\|\le\sqrt{\frac{2V(0)+g^2\rho^2\mu}{\lambda_{\min}(\mathbf{P})}} \tag{44}$$

which can explicitly describe that the bound of tracking error $\|\mathbf{e}\|$. If the initial state $V(0) = 0$, tracking error $\|\mathbf{e}\|$ can be made arbitrarily small by choosing adequate ρ. Equation (44) is very crucial to show that the proposed HOHNN controller will provide the closed-loop stability rigorously in the Lyapunov sense under the Assumption (19).

5. Simulation Results

An inverted pendulum on a cart depicted in Fig. 6 is presented to illustrate the

effectiveness of the proposed HOHNN controller. Consider the dynamics of the inverted pendulum which can be described as [11, 12]:

$$\ddot{\theta} = \frac{\frac{1}{2}ml\dot{\theta}^2 \sin(2\theta) - (m+M)g\sin(\theta)}{ml\cos^2(\theta) - \frac{4}{3}(m+M)l} - \frac{\cos(\theta)}{ml\cos^2(\theta) - \frac{4}{3}(m+M)l}u + d \qquad (45)$$

where θ is the angular position of the pendulum, m is the mass of the pendulum, M is the mass of the pendulum, d is the external disturbance, and l is the half the length of the pendulum. The values of variables are given in Table I.

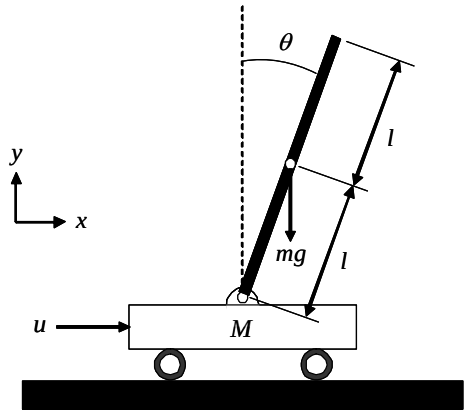

Fig. 6. Cart with an inverted pendulum.

TABLE I

DATA OF INVERTED PENDULUM ON A CART

m	mass of the pendulum	2 kg
M	Mass of the cart	8 kg
l	Half the length of the pendulum	0.5 m
g	acceleration due to gravity	9.81 m/s^2

Assume the system is free of external disturbance and the reference signal $\theta_r(t)$ is a sinusoid with the amplitude of $\pi/30$ in this example. The learning rates of weights are selected as $\eta_1 = 1.2$ and $\eta_2 = 1.0$; the slope of tanh(·) at the origin is selected as a = 1.0. The resistance and capacitance are chosen as $R = 5\Omega$ and $C = 0.005\text{F}$. Solving the Riccati-like equation in (23) for a choice of $\mathbf{Q} = 10\mathbf{I}$ and $\mathbf{k}_c = [2 \quad 1]^T$, we have $\mathbf{P} = \begin{bmatrix} 15 & 5 \\ 5 & 5 \end{bmatrix}$. There exist two neurons and one control input for the HOHNN controller. The three inputs $\varphi(u)$, e_1, and e_2 are combined to form the full input vector $\mathbf{Z} = \{\varphi(u) \quad e_1 \quad e_2 \quad \varphi(u)e_1 \quad \varphi(u)e_2 \quad e_1e_2\}$ which is fed into the HOHNN controller. The overall detailed structure for system control can be shown in

the following Fig. 7.

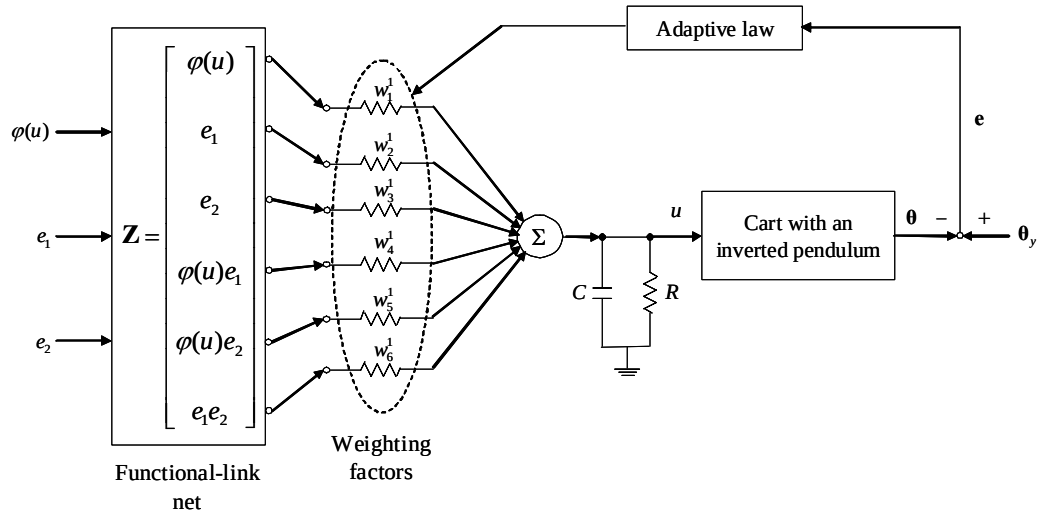

Fig. 7. The overall diagram of cart with an inverted pendulum using HOHNN controller.

To compare the HNN controller, the simulation results for the proposed HOHNN and HNN controllers with external disturbance $d = 2.5\sin(2t)$ when $t \geq 10$ second are shown in Figs. 8-13. This fact shows the strong disturbance-tolerance ability of the proposed HOHNN controller. Figure 8 shows the reference signal $\theta_r(t)$ and the actual pendulum angle $\theta(t)$. The enlarging drawing of Fig. 8 from $t = 9.5$ second to $t = 12.5$ second is shown in Fig. 9. Figure 10 shows the comparison of errors using HNN and HOHNN controllers and their enlarging drawing are shown in Fig. 11. The mean squared errors using HNN and HOHNN controllers and their enlarging drawing are shown in Fig. 12 and 13. From the simulation results, the HOHNN controller can result in better acceptable tracking performance than HNN controller.

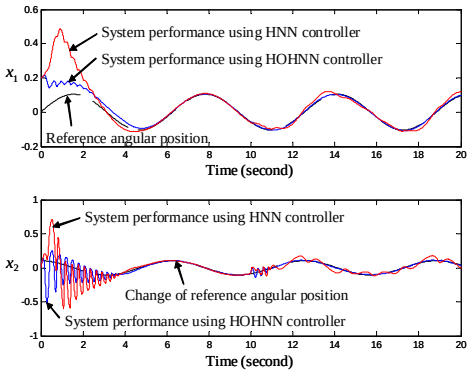

Fig. 8. Comparison of HNN and HOHNN controllers.

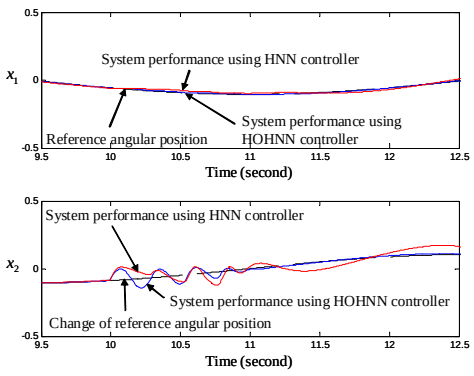

Fig. 9. Detail of Fig. 8 from t = 9.5 second to t = 12.5 second.

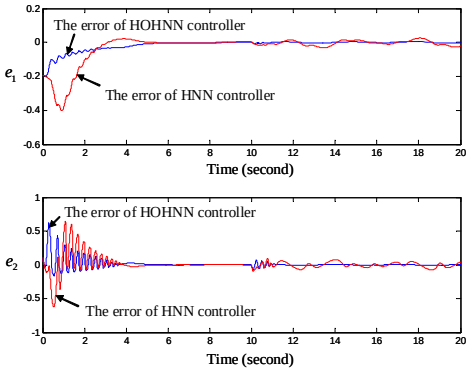

Fig. 10. Comparison of errors using HNN and HOHNN controllers.

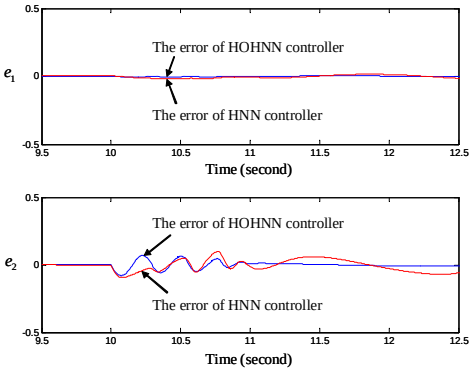

Fig. 11. Detail of Fig. 10 from t = 9.5 second to t = 12.5 second.

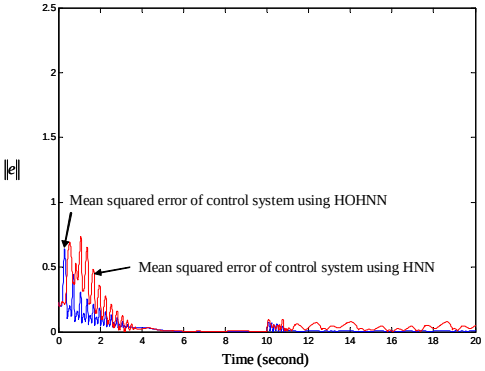

Fig. 12. The mean squared errors using HNN and HOHNN controllers.

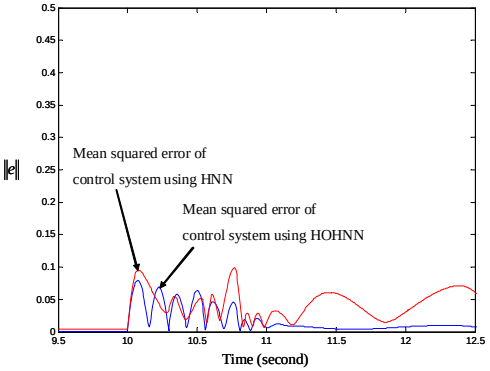

Fig. 13. Detail of Fig. 12 from $t = 9.5$ second to $t = 12.5$ second.

6. Conclusion

This paper has proposed a high-order Hopfield-based neural network (HOHNN) controller for the nonlinear dynamical systems. The simulation shows that HOHNN is capable of controlling the behavior of dynamical systems and the weighting matrices in HOHNN can be found via Lyapunov criteria. The adaptive laws to tune the weighting matrix can reduce the error between practical and reference state. The simulation results for HNN and HOHNN are finally conducted to show that the performance of HOHNN controller is better than HNN controller even though the nonlinear dynamical system encounters a disturbance suddenly.

Reference

[1] J. J. Hopfield, "Neural networks and physical systems with emergent collective computational abilities," *Proceedings of National Academy of Sciences*, USA, vol. 79, pp. 2554-2558, April 1982.

[2] Donq Liang, Lee, "Pattern Sequence Recognition Using a Time-Varying Hopfield Network," *IEEE Trans. Neural Networks*, vol. 13, no. 2, pp. 330-342, March 2002.

[3] Pajares, “A Hopfiled Neural Network for Image Change Detection,” *IEEE Trans. Neural Networks*, vol. 17, no. 5, pp. 1250-1264, Sep. 2006.

[4] Y. H. Pao, *Adaptive pattern Recognition and Neural Networks*, Addison-Wesley, Reading, 1989.

[5] Y. H. Pao, *Functional-link net computing: theory, system architecture, and functionalities*, Computer, 1992.

[6] Klassen, M. S. and Y. H. Pao, “Characteristics of the functional-link net: A higher order delta rule net,” *IEEE Proceedings of 2nd Annual International Conference on Neural Networks*, San Diago, CA, June 1995.

[7] Jagdish C. Patra, Ranendra N. Pal, B. N. Chatterji, and Ganapati Panda, “Identification of nonlinear dynamic systems using functional link artificial neural networks,” *IEEE Trans. System, Man, and Cybernetics-part B: Cybernetics*, vol. 29, no. 2, pp. 254-262, April 1999.

[8] Simon Haykin, *Neural Networks*, Upper Saddle River, NJ: Prentice-Hall, 1999.

[9] L. X. Wang, *Adaptive Fuzzy Systems and Control-Design and Stability Analysis*, Prentice-Hall, Englewood Cliffs, New Jersey, 1994.

[10] Y. G. Leu, W. Y. Wang, and T. T. Lee, “Observer-Based Direct Adaptive Fuzzy-Neural Control for Nonaffine Nonlinear Systems,” *IEEE Trans. Neural Networks*, vol. 16, no. 4, pp. 853-861, 2005.

[11] S. H. Zak, *Systems and Control*, New York: Oxford Univ. Press, 2003.

[12] R. H. Cannon Jr., *Dynamics of Physical Systems*, New York: McGraw-Hill, 1967.

參加國際學術會議心得報告

王啓旭

國立交通大學電機系特聘教授, IEEE Fellow

2010 IEEE International Conference on Networking, Sensing and Control

The 2010 IEEE International Conference on Networking, Sensing and Control was held in Chicago, 10-13, April, USA. The main theme of the conference is technologies and applications for wireless sensory networks. In recent years, wireless sensory networks have opened several areas of research and applications. Many companies and research agencies have started working on the next generation of these networks. Wireless sensory networks are now used in many fields such as homeland security, agriculture, energy management, intelligent transportation and traffic engineering, logistics, warehouse management, disaster management, healthcare delivery, military, smart buildings, and manufacturing. This conference provides a remarkable opportunity for the academic and industrial community to address new challenges and share solutions, and discuss future research directions in the area of wireless sensory networks.

The purpose for me and my PhD student to participate in this conference is to present the major content in this NSC research project. The title of this paper is:

"**Intelligent Adaptive Control of Uncertain Nonlinear Systems using Hopefield Neural Networks**"

This paper has also been submitted to IEEE Transactions on Control Systems Technology:, and is currently under minor revision. It is expected to be accepted by the end of 2010.

無衍生研發成果推廣資料

98 年度專題研究計畫研究成果彙整表

計畫主持人：王啟旭	計畫編號：98-2221-E-009-126-
計畫名稱：動態類神經網路在非線性系統鑑別與控制器設計之應用	

成果項目			量化			單位	備註（質化說明：如數個計畫共同成果、成果列為該期刊之封面故事...等）
			實際已達成數（被接受或已發表）	預期總達成數(含實際已達成數)	本計畫實際貢獻百分比		
國內	論文著作	期刊論文	0	0	100%	篇	
		研究報告/技術報告	0	0	100%		
		研討會論文	1	1	100%		
		專書	0	0	100%		
	專利	申請中件數	0	0	100%	件	
		已獲得件數	0	0	100%		
	技術移轉	件數	0	0	100%	件	
		權利金	0	0	100%	千元	
	參與計畫人力（本國籍）	碩士生	0	0	100%	人次	
		博士生	0	0	100%		
		博士後研究員	0	0	100%		
		專任助理	0	0	100%		
國外	論文著作	期刊論文	0	0	100%	篇	
		研究報告/技術報告	0	0	100%		
		研討會論文	0	0	100%		
		專書	0	0	100%	章/本	
	專利	申請中件數	0	0	100%	件	
		已獲得件數	0	0	100%		
	技術移轉	件數	0	0	100%	件	
		權利金	0	0	100%	千元	
	參與計畫人力（外國籍）	碩士生	2	0	100%	人次	
		博士生	1	0	100%		
		博士後研究員	0	0	100%		
		專任助理	0	0	100%		

其他成果 (無法以量化表達之成果如辦理學術活動、獲得獎項、重要國際合作、研究成果國際影響力及其他協助產業技術發展之具體效益事項等，請以文字敘述填列。)	無

	成果項目	量化	名稱或內容性質簡述
科教處計畫加填項目	測驗工具(含質性與量性)	0	
	課程/模組	0	
	電腦及網路系統或工具	0	
	教材	0	
	舉辦之活動/競賽	0	
	研討會/工作坊	0	
	電子報、網站	0	
	計畫成果推廣之參與（閱聽）人數	0	

國科會補助專題研究計畫成果報告自評表

請就研究內容與原計畫相符程度、達成預期目標情況、研究成果之學術或應用價值（簡要敘述成果所代表之意義、價值、影響或進一步發展之可能性）、是否適合在學術期刊發表或申請專利、主要發現或其他有關價值等，作一綜合評估。

1. 請就研究內容與原計畫相符程度、達成預期目標情況作一綜合評估

■達成目標

□未達成目標（請說明，以 100 字為限）

□實驗失敗

□因故實驗中斷

□其他原因

說明：

2. 研究成果在學術期刊發表或申請專利等情形：

論文：■已發表 □未發表之文稿 □撰寫中 □無

專利：□已獲得 □申請中 ■無

技轉：□已技轉 □洽談中 ■無

其他：(以 100 字為限)

3. 請依學術成就、技術創新、社會影響等方面，評估研究成果之學術或應用價值（簡要敘述成果所代表之意義、價值、影響或進一步發展之可能性）(以 500 字為限)

霍普菲爾神經網路屬於典型的動態類神經網路，神經網路中的權重值由李亞普諾夫穩定性理論來獲得，並以此保證系統的收斂性。本計劃探討高階霍普菲爾神經網路，其中經由函數型連結網路而得到每個神經元的額外輸入。相較於傳統的霍普菲爾網路，高階霍普菲爾網路呈現出較快的收斂速度。根據模擬結果可以明顯觀察到高階霍普菲爾網路控制器應用於非線性動態系統有較佳的效能。